THE JOURNAL OF BIOLOGICAL CHEMISTRY
Vol. 273, No. 27, Issue of July 3, pp. 17227–17235, 1998

Printed in U.S.A.

Conserved *in Vivo* Phosphorylation of Calnexin at Casein Kinase II Sites as Well as a Protein Kinase C/Proline-directed Kinase Site*

(Received for publication, April 15, 1998)

Hetty N. Wong‡, Malcolm A. Ward§, Alexander W. Bell‡, Eric Chevet‡¶, Satty Bains§, Walter P. Blackstock§, Roberto Solari§, David Y. Thomas‡‖, and John J. M. Bergeron‡ ‡‡**

*From the Departments of ‡Anatomy and Cell Biology and ‖Biology, McGill University, Montreal, Quebec H3A 2B2, Canada, **Biotechnology Research Institute, National Research Council of Canada, Montreal, Quebec H4P 2R2, Canada, and §Glaxo Wellcome Research and Development, Gunnels Wood Road, Stevenage, Hertfordshire SG1 2NY, United Kingdom*

Calnexin is a lectin-like chaperone of the endoplasmic reticulum (ER) that couples temporally and spatially *N*-linked oligosaccharide modifications with the productive folding of newly synthesized glycoproteins. Calnexin was originally identified as a major type I integral membrane protein substrate of kinase(s) associated with the ER. Casein kinase II (CK2) was subsequently identified as an ER-associated kinase responsible for the *in vitro* phosphorylation of calnexin in microsomes (Ou, W-J., Thomas, D. Y., Bell, A. W., and Bergeron, J. J. M. (1992) *J. Biol. Chem.* 267, 23789–23796). We now report on the *in vivo* sites of calnexin phosphorylation. After $^{32}PO_4$ labeling of HepG2 and Madin-Darby canine kidney cells, immunoprecipitated calnexin was phosphorylated exclusively on serine residues. Using nonradiolabeled cells, we subjected calnexin immunoprecipitates to in gel tryptic digestion followed by nanoelectrospray mass spectrometry employing selective scans specific for detection of phosphorylated fragments. Mass analyses identified three phosphorylated sites in calnexin from either HepG2 or Madin-Darby canine kidney cells. The three sites were localized to the more carboxyl-terminal half of the cytosolic domain: S^{534}DAE (CK2 motif), S^{544}QEE (CK2 motif), and S^{563}PR. We conclude that CK2 is a kinase that phosphorylates calnexin *in vivo* as well as in microsomes *in vitro*. Another yet to be identified kinase (protein kinase C and/or proline-directed kinase) is directed toward the most COOH-terminal serine residue. Elucidation of the signaling cascade responsible for calnexin phosphorylation at these sites *in vivo* may define a novel regulatory function for calnexin in cargo folding and transport to the ER exit sites.

Calnexin was originally identified and purified as a constituent of a complex of four co-isolated integral membrane proteins, two of which were phosphorylated in microsomes by ER[1]-associated kinase(s) (1). This phosphorylation was exclusively on serine residues and by controlled protease digestion found to be cytosolically oriented (1, 2). As a consequence of the cDNA cloning of this phosphoprotein, it was predicted and subsequently confirmed to be a type I integral membrane protein with extensive sequence similarity in its luminal domain to the ER luminal resident protein, calreticulin (1, 2). Calnexin and then calreticulin were found to be novel molecular chaperones of the ER. These chaperones act as lectins to couple oligosaccharide modifications to newly synthesized *N*-linked glycoproteins with productive glycoprotein folding. The lectin specificity of these chaperones has been identified as the recognition of high mannose oligosaccharides terminating in monoglucosyl residues linked α1–3 (3–13).

Purification of the ER-associated kinase that phosphorylated calnexin in microsomes led to the identification of CK2 (14). The properties of this kinase were consistent with the conditions that originally revealed calnexin phosphorylation (1, 14). Furthermore, purified CK2 has been found to phosphorylate calnexin on putative CK2 sites found within the cytosolic domain of calnexin (14, 15).

Calnexin is phosphorylated *in vivo* (16–18). Phosphorylated calnexin has been shown to associate with the null Hong Kong mutant of α-1-antitrypsin, coinciding with retention of this misfolded glycoprotein within the lumen of the ER (16). Phosphorylated calnexin was also found in association with newly synthesized major histocompatibility complex class I allotypes, which egressed from the ER at slow rates. Those allotypes transported to the Golgi apparatus at more rapid rates were associated preferentially with nonphosphorylated calnexin (17). Prolonged association of newly synthesized major histocompatibility complex class I heavy chains with calnexin was found in a B lymphoblastoid cell line transfected with HLA-B701 after incubation with the phosphatase inhibitor cantharidin or okadaic acid (19). Furthermore, when human synovial epithelial (McCoy) cells were treated with okadaic acid, the major cellular protein whose phosphorylation was shown to increase (based on two-dimensional gels followed by protein microsequencing) was calnexin (18). Remarkably, calnexin phosphorylation also increased 3-fold when McCoy cells were treated with *Clostridium difficile* cytotoxin B (18), a protein that glucosylates Rho proteins of the Ras superfamily (20).

Although some progress has been made on the kinases and sites of phosphorylation of calnexin after *in vitro* phosphorylation of intact microsomes (14, 15) little is known of the sites of calnexin phosphorylation *in vivo*. Here we report on their identification in two mammalian cell lines, HepG2 cells (human) and Madin-Darby canine kidney MDCK cells. Both cell lines

* This work was supported by grants from the Medical Research Council of Canada and Glaxo Wellcome (to J. J. M. B. and D. Y. T.). The costs of publication of this article were defrayed in part by the payment of page charges. This article must therefore be hereby marked "*advertisement*" in accordance with 18 U.S.C. Section 1734 solely to indicate this fact.

¶ Recipient of the postdoctoral fellowship from Association de Recherche Contre le Cancer.

‡‡ To whom correspondence should be addressed. Tel.: 514-398-6351; Fax: 514-398-5047; E-mail: eh14@musica.mcgill.ca.

[1] The abbreviations used are: ER, endoplasmic reticulum; CHAPS, 3-[(3-cholamidopropyl)dimethylammonio]-1-propanesulfonic acid; PAGE, polyacrylamide gel electrophoresis; FBS, fetal bovine serum; DE-MALDI, delayed extraction matrix-assisted laser desorption ionization; ToF, time of flight; MS, mass spectrometry; nano-ESI, nanoelectrospray ionization; CNL, constant neutral loss; TLC, thin layer cellulose; MS/MS, tandem mass spectrometry; CK2, casein kinase II; MDCK, Madin-Darby canine kidney; PKC, protein kinase C; PDK, proline-directed kinase; PVDF, polyvinylidene difluoride.

revealed phosphorylation of the cytosolic domain of calnexin exclusively on serine residues within CK2 motifs as well as a protein kinase C (PKC) and/or proline-directed kinase (PDK) motif.

EXPERIMENTAL PROCEDURES

Materials—Rabbit antibodies raised against a synthetic peptide, corresponding to amino acid residues 487–505 of canine calnexin, described previously were used (3). ^{32}P-Orthophosphoric acid (specific activity > 8000 Ci/mmol) was purchased from NEN Life Science Products. Protein A-Sepharose beads were from Amersham Pharmacia Biotech. Pyridine, phenylmethylsulfonyl fluoride, aprotinin, leupeptin, and HEPES were from Sigma. Sequencing grade bovine trypsin was from Boehringer Mannheim. TLC microcrystalline plates (0.1-mm thickness) were from EM Science (Gibbstown, NJ). Kodak XAR-5 OMAT film was purchased from Picker International Canada Inc. (Montreal, Quebec). Reagents for SDS-PAGE and protein determination were from Bio-Rad. All other reagents were from Sigma, Anachemia Canada Inc. (Lachine, Quebec), or Boehringer Mannheim.

Media and Cell Lines—Dulbecco's modified Eagle's medium, phosphate-deficient Dulbecco's modified Eagle's medium, dialyzed FBS, penicillin, and streptomycin were purchased from Life Technologies, Inc. FBS was obtained from HyClone Laboratories, Inc. (Logan, UT). Both human hepatoma (HepG2) cells and MDCK cells were cultured in Dulbecco's modified Eagle's medium supplemented with 10% (v/v) FBS, 500 units/ml penicillin, and 500 μg/ml of streptomycin. Cells were maintained in a 37 °C incubator with 5% atmospheric CO_2 and used when they were 80% confluent.

In vivo [^{32}P]O_4 Labeling of Cultured Cells and Immunoprecipitation—Cells were radiolabeled as described previously (16, 17) with the following modifications. Briefly, cells were washed in phosphate-free Dulbecco's modified Eagle's medium supplemented with 1% dialyzed FBS followed by incubation in the same medium for 1 h at 37 °C. Cells were then labeled by the addition of 2 mCi/ml [^{32}P]orthophosphate for 3 h. At the end of labeling, the cells were lysed as described previously (3). Briefly, cells were washed twice with ice-cold phosphate-buffered saline (20 mM $NaPO_4$, pH 7.5, 150 mM NaCl) and once with ice-cold HEPES-buffered saline (50 mM HEPES, pH 7.6, 200 mM NaCl) before harvesting. Cells were then lysed in 2% CHAPS/HEPES-buffered saline lysis buffer (2% (w/v) CHAPS, 1 mM phenylmethylsulfonyl fluoride, 10 μg/ml each leupeptin and aprotinin, 10 mM NaF, 10 mM $NaPP_i$, 0.4 mM $NaVO_4$, and 5 mM $NaMoO_4$) for 30 min on ice. The same procedures were used to immunoprecipitate calnexin from both ^{32}P-labeled and cold phosphate-labeled cellular extracts as described previously (3). Immunoprecipitated calnexin was isolated by SDS-PAGE. The gel was dried for 2 h at 80 °C under vacuum, or the proteins were transferred onto PVDF membrane (1). Radioactive bands were visualized by radioautography at room temperature.

Phosphoamino Acid Analysis—Phosphoamino acid analysis was performed as described (21). Briefly, *in vivo* phosphorylated calnexin was resolved by SDS-PAGE and electroblotted onto a PVDF membrane. ^{32}P-Labeled calnexin was detected by radioautography, and the corresponding PVDF bands were excised. The membrane containing phosphorylated calnexin was washed extensively with distilled water and subjected to acid hydrolysis, immersed in 6 N HCl at 110 °C for 60 min. The hydrolysate was transferred to a microcentrifuge tube, lyophilized, and dissolved in pH 1.9 buffer (88% formic acid, glacial acetic acid, H_2O; 2.5:7.8:89.7 (v/v/v)). Phosphoamino acid analysis was by two-dimensional electrophoresis on TLC plates in the presence of phosphoamino acid standards; phosphoserine, phosphothreonine, and phosphotyrosine. First dimension electrophoresis was carried out in pH 1.9 buffer for 20 min at 1.3 kV employing a Hunter thin layer electrophoresis system (C.B.S. Scientific, Del Mar, CA). Second dimension electrophoresis was carried out in pH 3.5 buffer (pyridine, glacial acetic acid, H_2O; 0.5:5:94.5 (v/v/v)) at 1.5 kV for 20 min. The standards were visualized by spraying a 0.25% (w/v) ninhydrin acetone solution followed by incubation at 65 °C for 10 min. The radiolabeled amino acids were detected by radioautography with an enhancing screen at −70 °C. Recovery from each step was monitored by Cerenkov counting.

In Gel Digestion and Mass Spectrometry (DE-MALDI MS and nano-ESI MS)—Calnexin immunoprecipitates from nonradiolabeled HepG2 and MDCK cell lysates were resolved by SDS-PAGE, visualized by Coomassie Blue staining (stain was 0.2% (w/v) Coomassie Brilliant Blue R250 in 50% (v/v) methanol in water containing 2% (v/v) acetic acid; destain was 50% (v/v) methanol in water containing 2% (v/v) acetic acid); and the corresponding gel slice was excised. Coomassie stain was removed by extraction (twice) with 50% (v/v) acetonitrile/H_2O, followed by two cycles each of extracting with acetonitrile and swelling with 100 mM NH_4HCO_3. Calnexin was in gel reduced and alkylated with 15 mM dithiothreitol and 1.3 mM iodoacetamide and then in gel digested with 13 μg/ml bovine trypsin in the presence of 5 mM $CaCl_2$ as described (22). Tryptic peptides were first extracted with acetonitrile, followed by two cycles each of swelling with 100 mM NH_4HCO_3 and extracting with acetonitrile and then two cycles each of swelling with 5% formic acid and extracting with acetonitrile. The efficiency of the extraction of calnexin tryptic phosphorylated fragments from gel pieces was evaluated with radiolabeled calnexin and Cerenkov counting. Greater than 70% of the radioactivity was extracted and recovered (data not shown). For DE-MALDI-ToF MS, dried peptide extracts were redissolved in 5% formic acid containing 5% methanol (10 μl) (22). An aliquot (0.4 μl) was spotted onto a stainless steel target precoated with α-cyano-4-hydroxycinnamic acid. The target was allowed to air dry before being washed with an aqueous solution containing 1% trifluoroacetic acid. Excess wash solution was blown off the target using compressed air. The target was loaded into the mass spectrometer for analysis by DE-MALDI-ToF

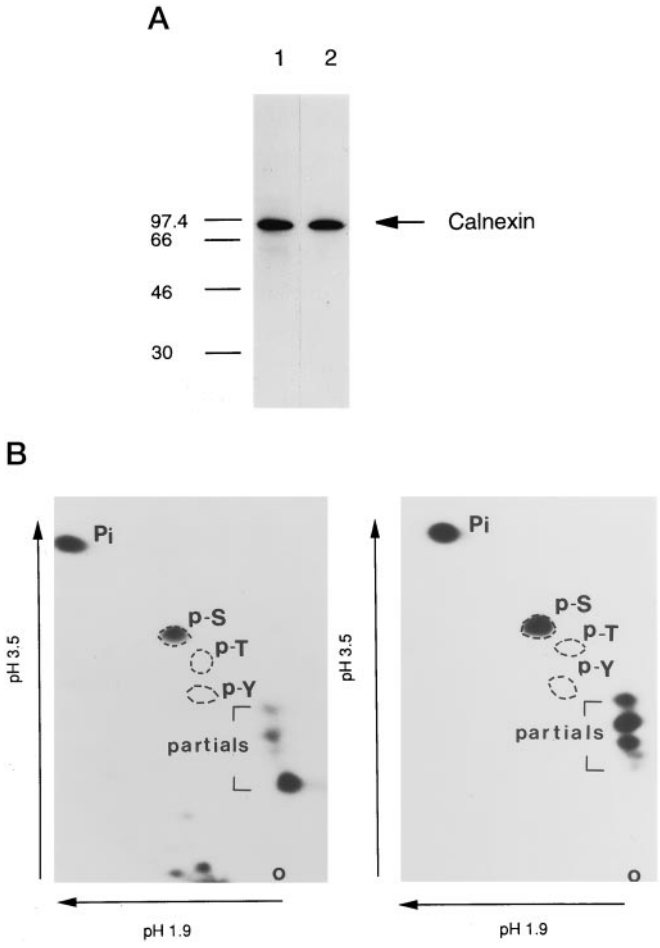

FIG. 1. **Calnexin is *in vivo* phosphorylated on serine residues.** HepG2 and MDCK cells were *in vivo* labeled with [^{32}P]orthophosphate for 3 h followed by lysis and immunoprecipitation of calnexin. The immunoprecipitates were resolved by 8% SDS-PAGE and transferred onto PVDF membranes. Phosphorylated calnexin was visualized by radioautography for 2 h at room temperature. *A*, SDS-PAGE-resolved ^{32}P-labeled calnexin from HepG2 cells (*lane 1*) and MDCK cells (*lane 2*). Calnexin is indicated on the *right*, and molecular weight standards are indicated on the *left*. ^{32}P-Labeled PVDF membrane-bound calnexin was subjected to phosphoamino acid analysis as described under "Experimental Procedures." *B*, phosphoamino acid analysis of calnexin from both HepG2 and MDCK cells (*left* and *right*, respectively) by TLC; first dimension electrophoresis in pH 1.9 buffer and second dimension electrophoresis in pH 3.5 buffer. The time of exposure was 68 h at −70 °C with an intensifying screen. The direction of electrophoresis toward the anode is indicated. The *dashed circles* indicate the positions of nonradiolabeled phosphoamino acid standards as visualized by ninhydrin staining. *o*, origin; *P-S*, phosphoserine; *P-T*, phosphothreonine; *P-Y*, phosphotyrosine; P_i, free phosphate and partials, products of incomplete peptide hydrolysis.

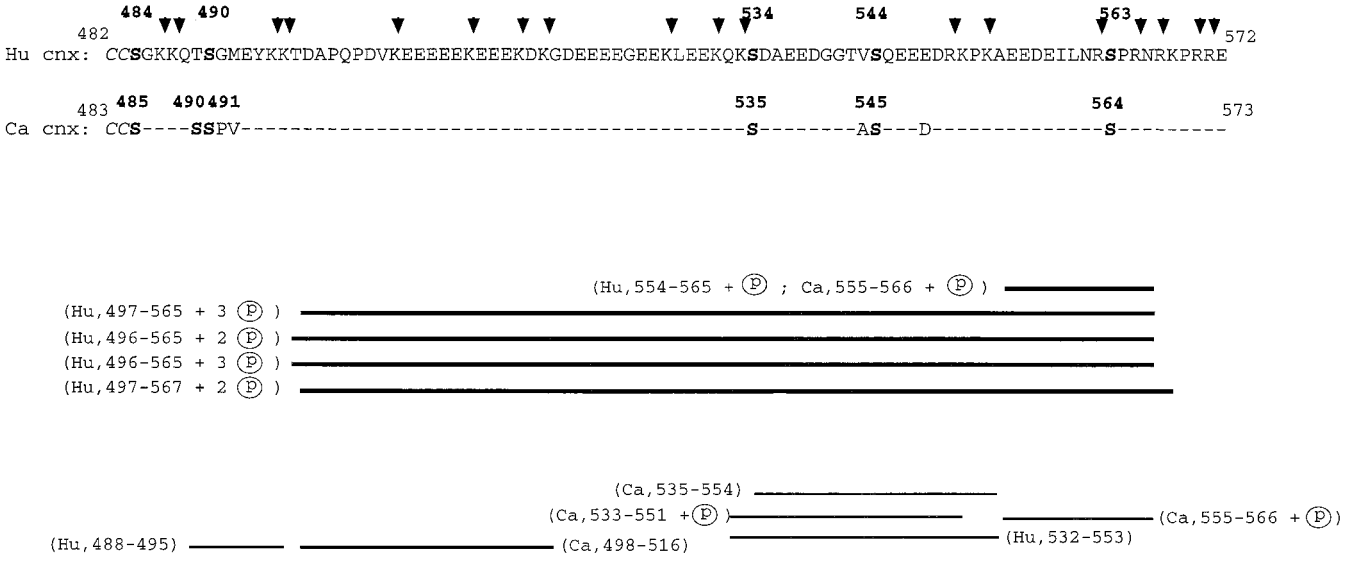

FIG. 2. **Sequence alignment of the cytosolic domains of canine and human calnexins and summary of cytosolic tryptic fragments characterized by MS.** *Top*, alignment of the cytosolic domains of human (amino acids 482–572) and canine (amino acids 483–573) calnexins. The *numbers* refer to the sequence of mature calnexin. *CC* (*italic type*), amino acid residues predicted to be the last two residues of the transmembrane domain; serine residues are in *boldface type*; five amino acid differences between human and canine calnexins *i.e.* Ser^{490}, Pro^{492}, Val^{493}, Ala^{544}, and Asp^{549} are shown for canine Cnx (*Ca cnx*), and identical amino acids are indicated by *dashes*. The *arrowheads* indicate the predicted sites of trypsin cleavage. *Bottom*, peptide fragments detected by DE-MALDI-ToF MS or Q1 nano-ESI MS are indicated by *thin solid lines*, and phosphorylated fragments identified by precursors *m/z* 79 or CNL scans are indicated by *thick solid lines*. *Hu* and *Ca* are the tryptic fragments detected from HepG2 and MDCK calnexins, respectively.

TABLE I
Potential serine phosphorylation site(s) of the cytosolic domains of calnexins

Parenthesis indicate motif residues that are not conserved between human and canine calnexins.

Canine calnexin[a]	Ser^{485}	Ser^{490}	Ser^{491}	Ser^{535}	Ser^{545}	Ser^{564}
CK2	−	−	+	+	+	−
PKC	+	−	−	−	−	+
PDK	−	−	(+)	−	−	+
PKA	−	(+)	−	−	−	−
Human calnexin[a]	**Ser^{484}**	**Ser^{490}**	**Ser^{534}**	**Ser^{544}**	**Ser^{563}**	
CK2	−	+	+	+	−	
PKC	+	−	−	−	+	
PDK	−	−	−	−	+	

[a] CK2, predicted casein kinase II site; PKC, predicted protein kinase C site; PDK, predicted proline-directed kinase site; PKA, predicted protein kinase A site.

mass spectrometry using a Bruker Reflex instrument fitted with a 337-nm nitrogen laser. All spectra were acquired with the instrument in reflector mode. Acquisition parameters were set as follows: sampling frequency, 500 MHz; gain, 50 mV; source voltage, 24,000 V; reflector voltage, 24850 V. DE-MALDI-ToF mass spectra were acquired for each digest and compared with mock in gel trypsin digest. Nano-ESI experiments were performed as described (23). Briefly, in gel trypsin-digested calnexin was desalted via a POROS R2 capillary column (22, 23) (PerSeptive Biosystems, Farmingham, MA); dried in a vacuum centrifuge; and resuspended in 10 μl of spraying solution (50% (v/v) methanol, 5% (v/v) ammonia in water for negative ion mode or 50% (v/v) methanol, 1% (v/v) formic acid in water for positive ion mode). 1 μl was inserted into a homemade capillary needle. Spraying capillary needles were made from borosilicate glass capillaries (Clark Electromedical Instruments, Pangbourne, Reading, UK) employing a micropipette puller (Sutter Instrument Co., Novato, CA), and gold was sputtered employing a vapor desorption instrument. A PE-Sciex API III triple quadrupole mass spectrometer (Perkin-Elmer) fitted with a nano-ESI source (24, 25) was used to acquire all electrospray mass spectra. The ion spray voltage was set to 600–650 V with an orifice potential of 60–70 V. Instrument polarity was set appropriate to the detection of positive or negative ions. Q1 scans were used to mass analyze ions relating to the intact peptides in the mixture. These were recorded by scanning the first quadrupole between *m/z* 400 and 2000 using a 1.0-ms dwell time and a 0.1-Da step size. Peptides containing phosphate produce a characteristic PO_3^- ion fragment at *m/z* 79 (26, 27). Molecular ions for these peptides were recorded by scanning the first quadrupole between *m/z* 300 and 1400 with the third quadrupole set to transmit *m/z* 79 only (precursors *m/z* 79 scans). Argon gas was used in the collision cell (quadrupole 2) at a collision gas thickness of 250 units. Scanning the first and third quadrupoles with an offset of *m/z* 49 profiled phosphopeptides by loss of H_3PO_4 (molecular mass of 98) from doubly charged molecular ions (Constant Neutral Loss scans) (28). For MS/MS detection, Q1 was set to transmit a mass window of 2 Da for product ion scans. Product ion spectra were accumulated with a 0.2-Da mass step size. Dwell time was 1.0 ms, and collision energy was optimized to obtain the MS/MS spectra. Spectra interpretation was performed using BioMultiView (Sciex) software.

Computer Analysis—Candidate kinases for the cytosolic serine residues of calnexin were predicted based on consensus sequence motifs employing the PROSITE data base of EXPASY[2] (29). Predicted peptide *m/z* values were evaluated employing tools provided by ProteinProspector.[3] Calnexin and calmegin sequence alignments were initially generated by BLASTp (30), FASTA (31), and MSA (32) and optimized manually.

RESULTS

Calnexin Is in Vivo Phosphorylated on Serine Residues in HepG2 and MDCK Cells—Calnexin was originally identified as a major substrate of ER-associated kinase(s) by *in vitro* phosphorylation of intact microsomes with [γ-^{32}P]GTP as phosphate donor (1). In order to determine the *in vivo* sites of phosphorylation for calnexin, both HepG2 and MDCK cells were *in vivo* labeled with [^{32}P]orthophosphate followed by immunoprecipitation with anti-calnexin antibodies. SDS-PAGE-resolved immunoprecipitates were electroblotted onto PVDF membranes and similar levels of phosphorylated calnexin from both cell types were revealed by radioautography (Fig. 1*A*, *lanes 1* and *2*). The bands corresponding to phosphorylated calnexin were excised from the PVDF membranes and subjected to phosphoamino acid analyses. Radioautograms of the two-dimensional TLC plates for both human and canine calnexins revealed only ^{32}P-labeled serine that comigrated with the nonradiolabeled phosphoserine standard as detected by ninhy-

[2] Available on the World Wide Web at http://expasy.hcuge.ch.
[3] Available on the World Wide Web at http://prospector.ucsf.edu.

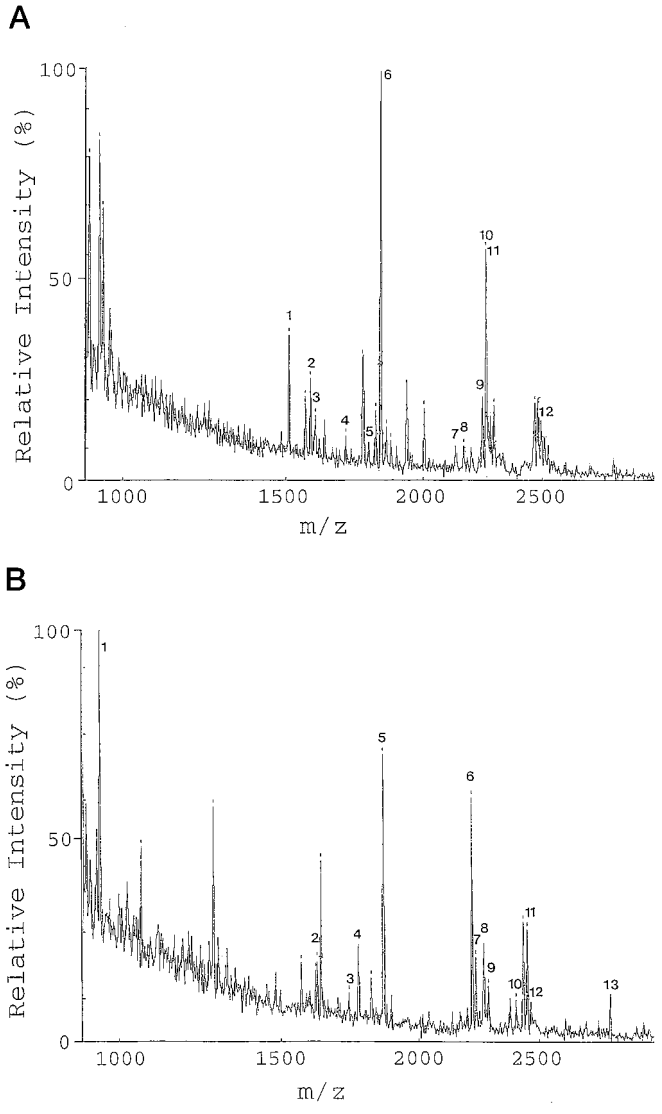

FIG. 3. **DE-MALDI-ToF mass analyses of tryptic fragments of calnexin.** Positive ion mode DE-MALDI-ToF mass spectra are shown for tryptic digests of calnexin from MDCK (*A*) and HepG2 (*B*). The identities of the numbered peaks are shown in Table II. The *x* axis indicates the mass-to-charge (*m/z*) values, and the *y* axis indicates the relative ion intensity.

drin staining (*left* and *right parts* of Fig. 1*B*, respectively). The phosphorylated residues were not altered with longer (up to 24 h) *in vivo* radiolabeling (data not shown). Hence, calnexin was exclusively *in vivo* phosphorylated on serine residues in both cell types.

In isolated ER microsomes, *in vitro* phosphorylation by ER-associated kinase(s) is exclusively on the cytosolic domain of calnexin (1). The cytosolic COOH-terminal domains of canine (MDCK) and human (HepG2) calnexins (1, 33) share 94% identity (Fig. 2). The cytosolic domain of canine calnexin contains six serines, and the cytosolic domain of human calnexin contains five equivalent serines and a threonine. The five conserved cytosolic serine residues are in primary sequence motifs that are predicted to be recognized by CK2 (34), PKC (35, 36), PDK (37, 38), or protein kinase A (39, 40) (Table I). To identify the *in vivo* sites of phosphorylation of calnexin we proceeded to mass spectrometry.

Analyses of Tryptic Digests of Calnexin by DE-MALDI-ToF MS—Calnexin was immunoprecipitated from nonradiolabeled cell lysates from both cultured MDCK and HepG2 cells. After separation by SDS-PAGE and visualization by Coomassie

TABLE II

Summary of DE-MALDI-ToF mass spectral data (Fig. 3, A and B)

The observed masses and calculated monoisotopic (Mi) and average masses for specific monoprotonated tryptic fragments ($[M + H]^+$) from MDCK and HepG2 calnexins are shown.

Peak	Observed mass	Calculated		Residues	Modification[a]
		Mi mass	Average mass		
MDCK (Fig. 3*A*)					
1	1508.76	1508.67	1509.5	555–566	1 PO_4
2	1584.85	1584.76	1585.8	175–186	
3	1602.86	1602.79	1603.8	427–440	
4	1707.75	1707.83	1708.9	383–396	
5	1811.76	1811.87	1812.9	69–84	
6	1835.90	1835.92	1837.1	382–396	
7	2130.90	2129.78	2130.9	533–551	Pyro-Q, 1 PO_4
8	2163.98	2163.93	2165.2	535–554	
9	2240.14	2240.14	2241.6	364–381	
10	2254.86	2255.01	2256.4	256–273	
11	2259.10	2259.01	2260.3	498–516	
12	2479.04	2479.10	2480.8	341–361	
HepG2 (Fig. 3*B*)					
1	943.42	943.42	944.1	488–495	
2	1616.84	1616.81	1617.8	426–439	
3	1735.87	1735.83	1736.9	382–395	
4	1770.87	1770.83	1771.9	42–57	
5	1863.93	1863.93	1865.1	381–395	
6	2213.09	2213.13	2214.6	363–380	
7	2229.12	2229.13	2230.6	363–380	Met-ox
8	2262.14	2262.11	2263.5	38–57	
9	2283.05	2283.05	2284.4	255–272	
10	2398.31	2398.25	2399.8	361–380	
11	2447.24	2447.12	2448.8	340–360	
12	2462.14	2462.13	2463.5	532–553	
13	2813.14	2813.42	2815.2	42–67	

[a] PO_4, phosphate group; Met-ox, methionine sulfoxide; pyro-Q, pyroglutamic acid.

staining, calnexin was in gel digested with trypsin as described under "Experimental Procedures." DE-MALDI-ToF mass spectra for the tryptic peptides of calnexin from MDCK and HepG2 were collected (Fig. 3, *A* and *B*). Peptide masses not observed in the mock in gel digest (data not shown), were employed to confirm the identity of MDCK and HepG2 calnexins. Total coverage for calnexin from MDCK cells was 165 of 573 (28.8%) amino acid residues, and coverage from HepG2 cells was 171 of 572 (29.9%) amino acid residues. With respect to the cytosolic domain of calnexin, however, the degree of coverage was 58.4 and 33.7% from MDCK and HepG2 cells, respectively. This coverage by DE-MALDI-ToF included phosphopeptides observed as peak 1 and peak 7 in Fig. 3*A* for MDCK calnexin and as summarized in Table II. Coverage of the cytosolic domain was increased by nano-ESI MS and was greater than 90% by combination of both mass spectrometric techniques (see below). Poor coverage of the luminal domain was consistent with the generation of a protease-resistant core in the presence of Ca^{2+} (2), conditions employed during in gel trypsin digestion.

Analyses of Tryptic Digests of Calnexin by Nano-ESI MS: Identity and in Vivo Sites of Phosphorylation—The Q1 positive ion spectrum between *m/z* 800 and 1150 of HepG2 calnexin tryptic digests displays four ions (P1–P4) tentatively assigned as tryptic fragments of calnexin by comparison with mock in gel trypsin digest (Figs. 4, *A* and *B*). By comparison of the observed masses and the cDNA predicted calculated average masses (33), P1 (*m/z* 817) and P2 (*m/z* 886.3) correspond to the doubly positively charged states of the tryptic fragments ^{91}ESKLPGDKGLVLMSR^{105} (calculated average mass, 1631.0 atomic mass units) and ^{42}APVPTGEVYFADSFDR^{57} (calculated average mass, 1771.9 atomic mass units), respectively, of calnexin. The P3 (*m/z* 903) and P4 (*m/z* 910) ions correspond to the triply positively charged states of the tryptic fragments ^{151}TPELNLDQFHDKTPYTIMFGPDK^{173} (calculated average mass,

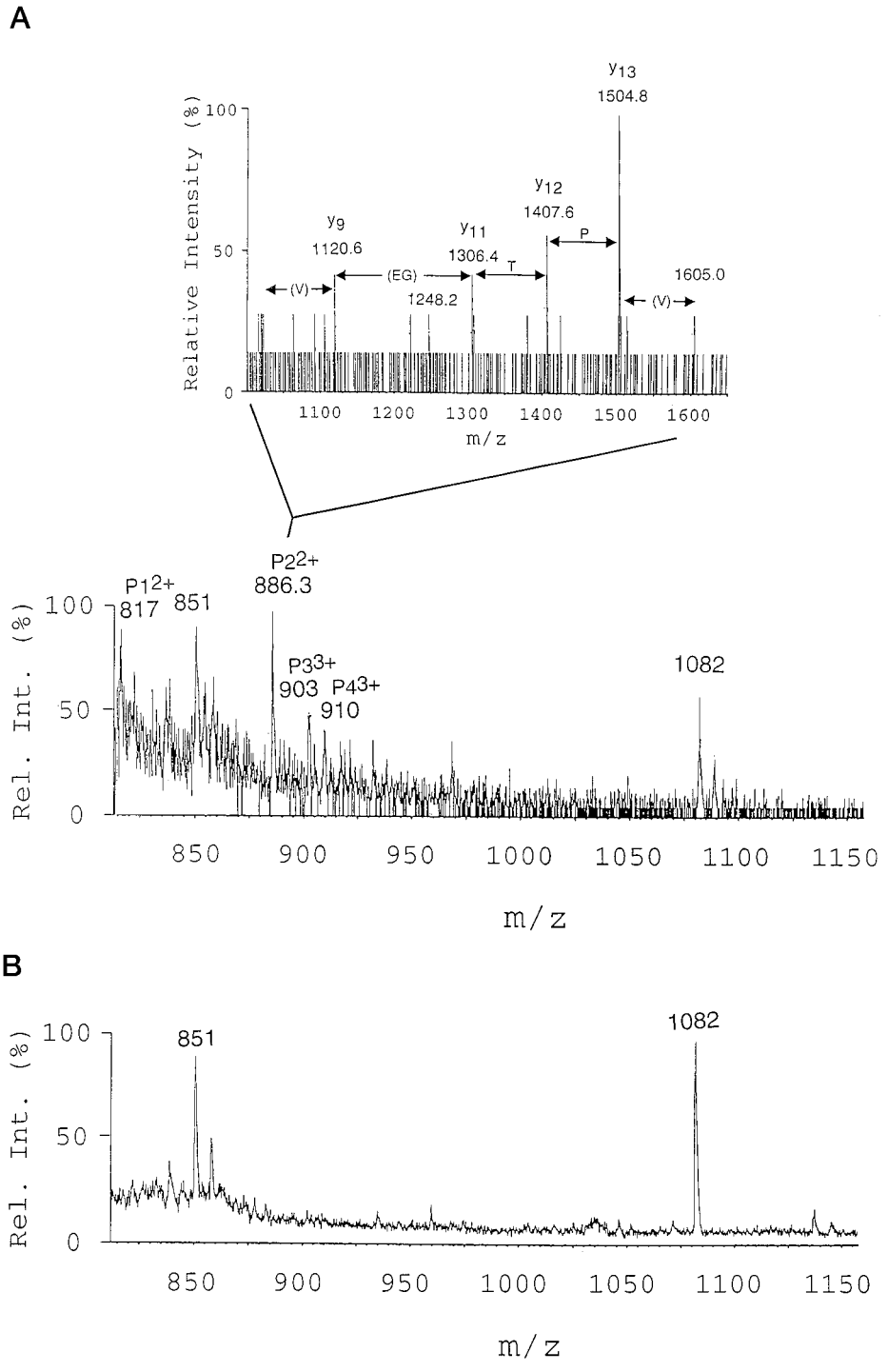

FIG. 4. **Nano-ESI MS and MS/MS of tryptic fragments of calnexin.** *A* and *B*, positive ion Q1 scans (800–1150 *m/z*) of calnexin and mock in gel tryptic digest, respectively. The identities of the labeled peaks are as follows: P1 (*m/z* 817), the +2 charged tryptic fragment of ^{91}ESKLPGDKGLVLMSR^{105} (calculated average mass, 1631.0 amu); P2 (*m/z* 886.3), the +2 charged tryptic fragments of ^{42}APVPTGEVYFADSFDR^{57} (calculated average mass, 1771.9 atomic mass units); P3 (*m/z* 903), the +3 charged tryptic fragment of ^{151}TPELNLDQFHDKTPYTIMFGPDK^{173} (calculated average mass, 2709.1 atomic mass units); and P4 (*m/z* 910), the +3 charged tryptic fragment of ^{191}TGIYEEKHAKRPDADLKTYFTDK^{213} (calculated average mass, 2728.0 atomic mass units) of HepG2 calnexin. *Inset*, positive ion MS/MS profile of *m/z* 886.3 (P2), identifying the y ion series corresponding to . . . (V)PT(GE)(V) . . . (weak assignments identified by parentheses; see "Results"). The *x* axis indicates the mass-to-charge (*m/z*) values, and the *y* axis indicates the relative ion intensity.

2709.1 atomic mass units) and ^{191}TGIYEEKHAKRPDADLKTYFTDK^{213} (calculated average mass, 2728.0 atomic mass units), respectively, of calnexin. The tentative assignment of the major non-trypsin tryptic peptide ion P2 (*m/z* 886.3) was confirmed by generation of sequence-specific sequence tags by MS/MS. Prominent peptide fragment ions of 1120.6, 1306.4, 1407.6, and 1504.8 *m/z* values correspond to y-ion series of singly positively charged ions, y_9 (calculated *m/z* 1120.2), y_{11} (calculated *m/z* 1306.4), y_{12} (calculated *m/z* 1407.5), y_{13} (calculated *m/z* 1504.6) for collision-induced fragmentation of the calnexin tryptic peptide ^{42}APVPTGEVYFADSFDR^{57} (using ProteinProspector search tools). This identification is unambiguous (search parameters: mass tolerance of 0.5 Da for both parent and fragmented ions using ProteinProspector tools), and the partial sequence . . . (Val^{44})-Pro-Thr-(Gly-Glu)-(Val^{49}) . . . (weak assignments shown in parentheses) can be assigned from the MS/MS spectrum, taking into account potential weak signals for y_8 (calculated *m/z* 1021.1), y_{10} (calculated *m/z* 1249.3) and y_{14} (calculated *m/z* 1603.7) (Fig. 4, *inset*).

Only two phosphopeptides were detected by DE-MALDI-ToF MS (Table II). Hence, we proceeded to characterize in greater detail the phosphorylated peptides in the desalted total tryptic digests of nonradiolabeled phosphocalnexin from both MDCK and HepG2 cells employing two selective techniques for identification of phosphorylated fragments: scans for precursors *m/z* 79 in negative ion mode (26, 27) or scans for constant neutral loss (CNL) of H_3PO_4 (*m/z* 49 for doubly charged peptides) in positive ion mode (28). Precursors *m/z* 79 scans reveal

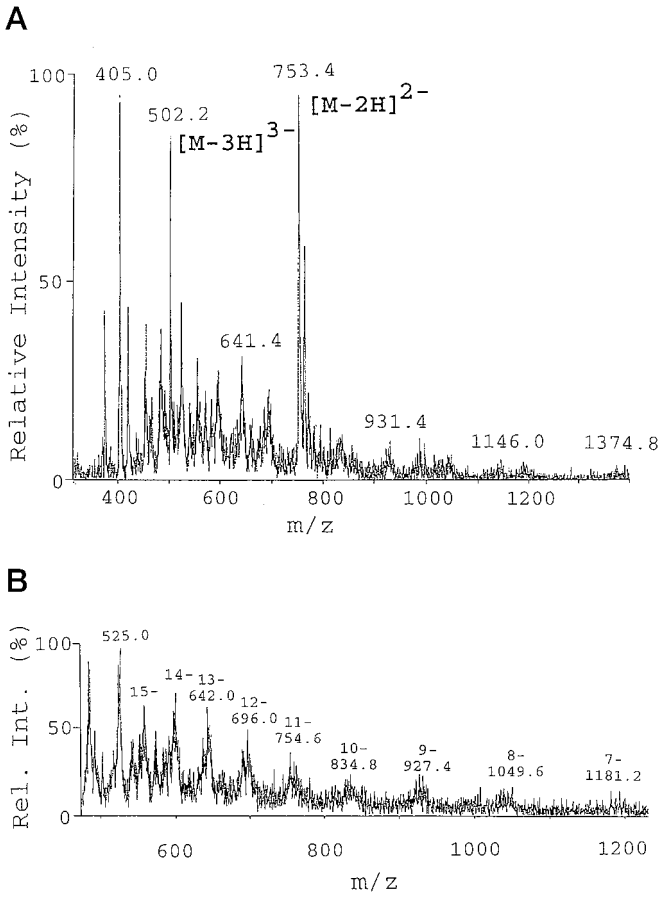

FIG. 5. **Precursors *m/z* 79 mass analyses of phosphorylated tryptic fragments of calnexin.** *A* and *B*, precursors *m/z* 79 negative ion scans of the tryptic peptides of calnexin from MDCK and HepG2 cells, respectively. Precursor ions that fragment to produce an ion at *m/z* 79 (PO_3^-) are detected. The −3 ($[M - 3H]^{3-}$; 502.2 atomic mass units) and −2 ($[M - 2H]^{2-}$; 753.4 atomic mass units) charged states of the phosphorylated fragment ^{555}AEEDEILNR**pS**PR^{566} (calculated average mass, 1509.5 atomic mass units) (*A*) and the multiply charged states of the clustered ion series (*B*) are indicated. The *x* axis indicates the mass-to-charge (*m/z*) values, and the *y* axis indicates the relative ion intensity.

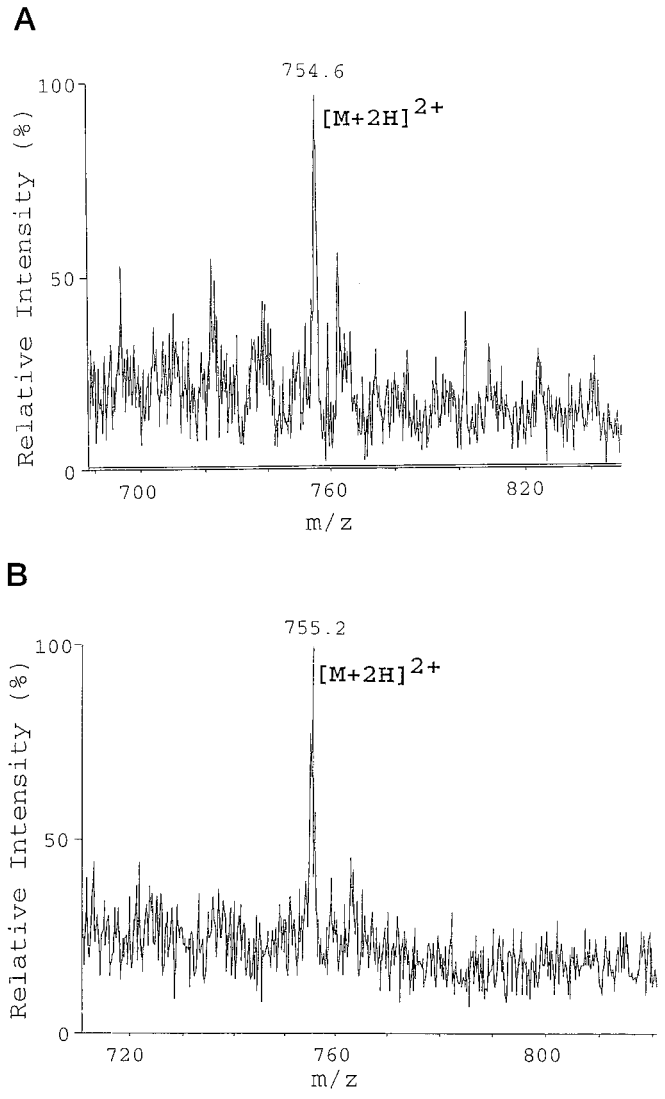

FIG. 6. **Constant neutral loss mass analyses of phosphorylated calnexin tryptic fragments.** *A* and *B*, CNL scans of the tryptic peptides of MDCK and HepG2 calnexins, respectively. Precursor ions that fragment to lose a neutral fragment equivalent to *m/z* 49 are detected for doubly charged peptides. The peptide ions, $[M + 2H]^{2+}$, with the *m/z* values of 754.6 or 755.2, correspond to the doubly positively charged phosphorylated tryptic peptide, AEEDEILNRpSPR (calculated average mass, 1509.5 atomic mass units), of MDCK (555–566) or HepG2 (554–565) calnexin. The *x* axis indicates the mass-to-charge (*m/z*) values, and the *y* axis indicates the relative ion intensity.

precursor ions that fragment to produce a characteristic product ion of *m/z* 79 that corresponds to the phosphate anion, PO_3^-. CNL scans reveal the masses of parent ions that lose the phosphate group, H_3PO_4 (molecular mass of 98), as a neutral fragment. A loss of *m/z* 49 would be observed from doubly charged precursor ions, $[M - H_3PO_4 + 2H]^{2+}$.

Precursors *m/z* 79 scans of the tryptic peptides from MDCK calnexin were dominated by three major phosphorylated peptide ions (Fig. 5*A*). Two of the three *m/z* values (753.4 and 502.2) correspond to the doubly and triply negatively charged states of the phosphorylated tryptic fragment ^{555}AEEDEILNR**pS**PR^{566} (where pS represents phosphoserine; calculated average mass, 1509.5 atomic mass units). The ion at *m/z* 405.0 is a commonly observed nonspecific background peak.[4] CNL *m/z* 49 scans of the tryptic fragments of MDCK calnexin (Fig. 6*A*) confirmed the former assignment, since the doubly charged phosphopeptide ^{555}AEEDEILNR**pS**PR^{566} (*m/z* 754.6) was observed.

Mass spectral analyses of the tryptic peptides from HepG2 calnexin by precursors *m/z* 79 scans revealed a clustered series of multiply charged ions (Fig. 5*B*) that upon deconvolution identified several large phosphorylated partial tryptic fragments derived from the cytosolic domain of HepG2 calnexin (see below). Analyses of this tryptic digest of HepG2 calnexin by CNL *m/z* 49 scans detected a $[M + 2H]^{2+}$ peptide ion with an *m/z* value of 755.2 (Fig. 6*B*), equivalent to the fragment similarly observed for MDCK calnexin (Fig. 6*A*). This fragment was not observed as strongly by precursors *m/z* 79 scans of the trypsinized HepG2 calnexin as it was observed for trypsinized MDCK calnexin (Fig. 5, compare *A* and *B*). The selectivity of the CNL *m/z* 49 scans, however, confirmed the presence of this same fragment ^{554}AEEDEILNR**pS**PR^{565} in the HepG2 calnexin tryptic digest.

The clustered series of multiply charged ions recorded by precursors *m/z* 79 scans of trypsinized HepG2 calnexin was subjected to deconvolution employing the Hypermass Reconstruction software (41). The reconstruct algorithm was initially carried out over the range of 2,000–10,000 Da and then focused in on the range of interest. No discernible species could be identified at other masses. The reconstruct profile (Fig. 7)

[4] M. A. Ward, unpublished observations.

indicated that the clustered series of multiply charged ions was derived from partial digests of the same phosphorylated region of the cytosolic domain of HepG2 calnexin. The partial tryptic fragments (Fig. 7) corresponded to the region K^{496} T^{497}DAPQPDVKEEEEEKEEEKDKGDEEEEGEEKLEEKQK**S**DAEEDGGTV**S**QEEEDRKPKAEEDEILNR**S**PR^{565}NR^{567} of calnexin (boldface type represents potential sites of phosphorylation). The observed masses and their calculated monoisotopic and average masses are tabulated (Fig. 7). These phosphorylated partial tryptic fragments contained three of the five serine residues, Ser^{534}, Ser^{544}, and Ser^{563}, of the cytosolic domain of human calnexin, and these fragments contained either two or three phosphate groups. Thus, these three serine residues represent the *in vivo* phosphorylation sites for calnexin. Close inspection of the precursors *m/z* 79 scans for phosphorylated trypsinized MDCK calnexin revealed a similar clustered series of multiply charged ions (Fig. 5, *A* and *B*), albeit these signals were weaker relative to the dominant ions (*m/z* 405.0, 502.2, and 753.4) but consistent with those observed in Fig. 5*B*. Partial digestion of phosphorylated MDCK calnexin was probably

	Obs. Mass	Cal. Mi Mass	Cal. Av.Mass
Peak 1: 497-565 + 3 HPO_3	8224.0	8225.6	8230.3
Peak 2: 496-565 + 2 HPO_3	8278.0	8273.7	8278.4
Peak 3: 496-565 + 3 HPO_3	8356.0	8353.7	8358.4
Peak 4: 497-567 + 2 HPO_3	8415.0	8415.8	8420.5

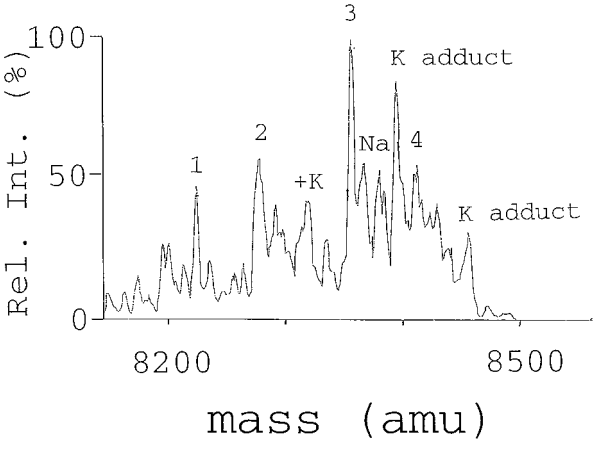

FIG. 7. **Reconstruct profile of precursors *m/z* 79 scans of HepG2 calnexin.** Deconvolution of the clustered series of multiply charged ions of HepG2 calnexin (Fig. 5*B*) employing the Hypermass reconstruction software (41). The identities of the numbered fragments are tabulated. Na^+ and K^+ adducts are indicated. *mi*, monoisotopic; *av*, average. The *x* axis indicates the mass values (atomic mass units (*amu*)), and the *y* axis indicates the relative ion intensity.

prevalent but to a lesser extent in this sample. Attempts to deconvolute these clusters of multiply charged ions (Fig. 5*A*) were unsuccessful due to the strong signals from the three abundant ions. Differences in sensitivity to trypsinization is unclear. As a precaution to autodigestion, trypsinization was performed in the presence of 5 mM Ca^{2+} (22, 23). This precaution may have contributed to an increased proteolytic resistance of the cytosolic domain, since Ca^{2+} binds to this domain (42). This caveat is similar to that indicated above for poor coverage of the luminal domain (Fig. 3, *A* and *B*), resulting from an increased proteolytic resistance induced by millimolar concentrations of Ca^{2+} (2). Nevertheless, these data are consistent with MDCK calnexin being phosphorylated on the equivalent three serine residues, *i.e.* Ser^{535}, Ser^{545}, and Ser^{564} (summarized in Fig. 8).

DISCUSSION

A recently uncovered family of resident ER proteins has revealed properties of novel lectin-like molecular chaperones. These recognize *N*-linked glycoproteins and couple *N*-linked oligosaccharide modification with productive glycoprotein folding (3–13, 43). The family is composed of calnexin, a type I transmembrane protein of the ER (1, 2); calreticulin, a KDEL-terminated soluble ER-resident protein (44); and calmegin, a testis-specific ER transmembrane protein with sequence conservation at the predicted luminal domain (45).

Major differences among the three proteins are found at their COOH termini. Mammalian calnexins reveal 89 cytosolically oriented residues (1, 2, 33, 42), which were here shown to be phosphorylated at three of the four invariant serine residues. The calmegin deduced protein sequences predict 119 amino acids cytosolically oriented (45, 46) with six conserved (human and mouse) potential serine phosphorylation sites. The calmegin conserved potential serine phosphorylation sites are, as with the observed sites of serine phosphorylation in calnexin, also in the COOH-terminal half of the respective cytosolic domain. Five of the six potential serine phosphorylation sites of calmegin are within motifs similar to those observed for calnexin; three are in CK2 motifs, one is in a PKC motif, and another (mouse sequence only) is in a PDK motif (Fig. 9). Thus, calmegin is predicted to be phosphorylated on equivalent serines to those in calnexin (Fig. 9). The alignment of the cytosolic domains of calnexins and calmegins identifies three major (and three minor) loops (*boxed* in Fig. 9) that are unique to the calmegins. Furthermore, this alignment reveals that the cytosolic domains of both calnexin and calmegin can be divided into four subdomains: a juxtamembrane basic, lysine-rich subdomain; a central acidic, glutamic acid-rich subdomain; a phosphorylation signaling subdomain; and a putative COOH-termi-

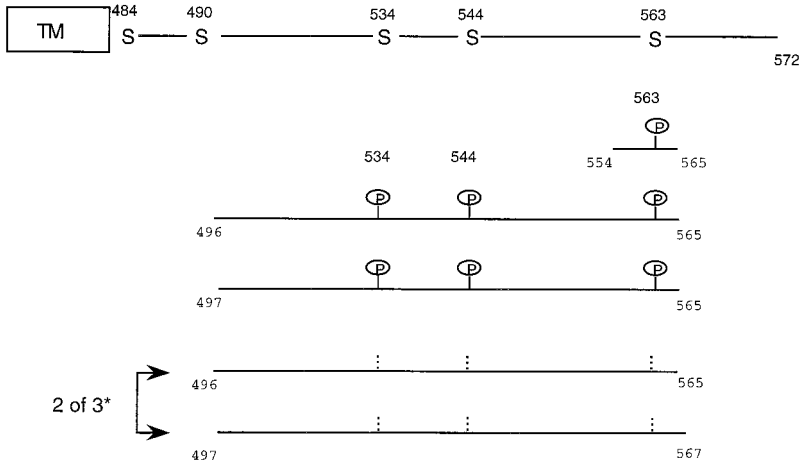

FIG. 8. **Schematic representation of *in vivo* phosphorylation sites of calnexin.** The cytosolic domain of HepG2 (human) calnexin is presented. Phosphorylated fragments detected either by precursors *m/z* 79 or CNL scans of either HepG2 or MDCK calnexin are indicated. The *numbering* indicates amino acid residues of mature human calnexin. Two diphosphorylated peptides (496–565 and 497–567, see Fig. 7) that contain three potential serine phosphorylation sites are indicated by *2 of 3**.

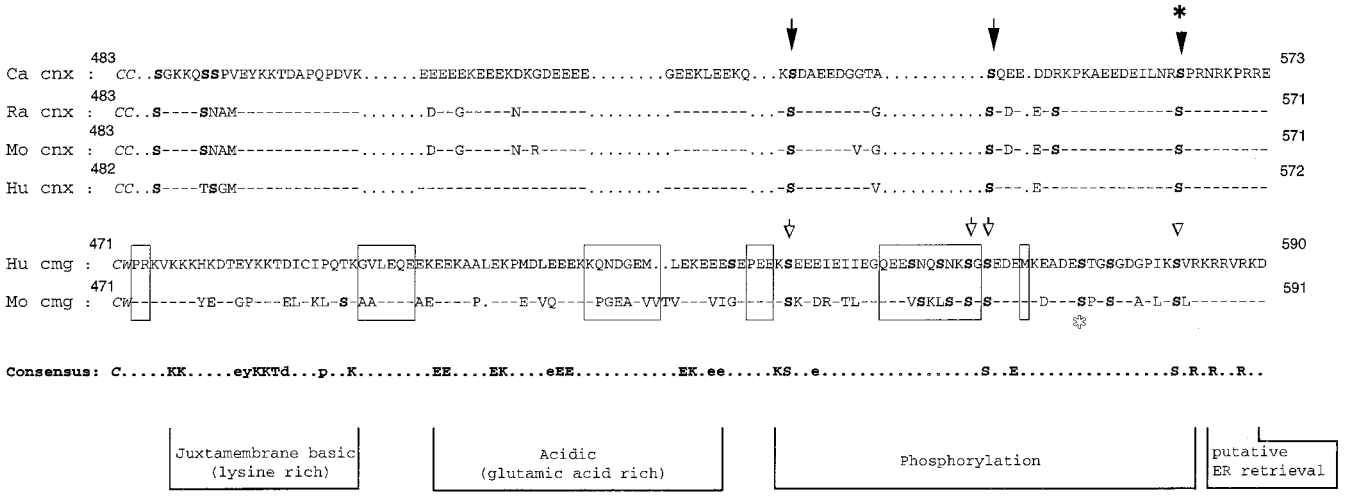

FIG. 9. **Sequence alignment of the cytosolic domains of known mammalian calnexins and calmegins.** Predicted cytosolic domains of canine (*Ca*; Refs. 1 and 14), rat (*Ra*; Ref. 42), mouse (*Mo*; Ref. 42), and human (*Hu*; Ref. 33) calnexins (*cnx*) and human and mouse calmegins (*cmg*; Refs. 45 and 46) are shown. *CC* and *CW* (*italic type*), amino acid residues predicted to be the last two residues of the transmembrane domains of calnexin and calmegin, respectively. Calnexin identified (*closed symbols*) and calmegin putative (*open symbols*) phosphorylation sites are shown. Potential kinases are as follows: CK2 (*arrows*), PKC (*arrowheads*), and PDK (*asterisks*). Residue *numbers* refer to the mature calnexins or calmegins. Serine residues are in *boldface type*; amino acid differences among the calnexins and among the calmegins are indicated; and identities are indicated by *dashes*. Gaps introduced to optimize alignments are shown as *dots*. Calnexin alignment identifies two deletions of one amino acid at position 507 and 524 of rodent calnexins; similarly, calmegin alignment identifies two deletions of one (*Mo*, 510) or two (*Hu*, 528) amino acids. Calnexin/calmegin alignment identifies six deletions/insertions of 2, 6, 8, 3, and 11 residues and 1 residue (*enclosed boxes*, calmegin). Consensus sequence is as follows: invariant (*boldface uppercase type*) and five of six identities (*bold lowercase type*). *Boldface dots* indicate differences. The four subdomains (*i.e.* the juxtamembrane basic, acidic, phosphorylation, and the predicted ER retrieval (47) domains) are indicated.

nal ER retrieval subdomain (47) (Fig. 9). Calreticulin is a luminal ER-resident protein that has no cytosolically oriented sequences but rather a COOH-terminal KDEL ER retrieval signal (48).

For yeast, greater evolutionary divergence has occurred at the cytosolic domain of calnexin as opposed to the intraluminal domain. The 48-amino acid cytosolic domain of the calnexin homologue Cnx1 in the fission yeast, *Schizosaccharomyces pombe*, is phosphorylated *in vivo*.[5] The *S. pombe* calnexin gene is essential for viability, but the cytosolic domain is dispensable for that essential feature (49). The *Saccharomyces cerevisiae* calnexin homologue Cne1p reveals only one potential cytosolic amino acid (Thr^{482}), and this calnexin gene, *CNE1*, is nonessential for *S. cerevisiae* viability (50). The riddle of the evolution of a cytosolic domain for *S. pombe* calnexin coincident with essential function(s) for viability for which the cytosolic domain appears to be dispensable may be ultimately resolved by an analysis of the signaling cascades that phosphorylate calnexin in mammalian species and in *S. pombe*.[5]

The cytosolic domains of all known mammalian calnexins display 83% identity with four invariant serines (Fig. 9). As a consequence of this high degree of sequence identity, we set out to identify the sequences constitutively phosphorylated in two cell lines, *i.e.* human HepG2 and canine MDCK cells. By phosphoamino acid analyses, both calnexins were exclusively *in vivo* phosphorylated on serine residues.

The first cytosolic serine residue, Ser^{484} and Ser^{485} of HepG2 and MDCK calnexins, respectively, is a juxtamembrane serine residue that is invariant among mammalian calnexins (Fig. 9) and corresponds to a potential PKC phosphorylation site. A tryptic peptide containing the transmembrane domain and thus the juxtamembrane serine residue was not detected by MS analyses. Low recovery of this tryptic fragment may be due to poor extractability (51) of such a peptide and/or due to partial proteolysis generating very large hydrophobic poorly extractable fragments probably linked to the protease-resistant Ca^{2+} luminal core of calnexin (2). The next COOH-terminal serine residue was conserved in HepG2 (Ser^{490}, a potential CK2 phosphorylation site) and MDCK (Ser^{491}, a potential CK2/PDK phosphorylation site) calnexins but not rodent calnexins (Fig. 9). This site was detected only as a nonphosphorylated fragment by MS analysis of the HepG2 tryptic digests (Fig. 3*B*).

As summarized in Fig. 8, only Ser^{534}, Ser^{544}, and Ser^{563} (human numbering, invariant in mammalian calnexins; see Fig. 9) were *in vivo* phosphorylated as detected by two selective nano-ESI MS techniques for detection of phosphorylated peptides. Two of these three invariant serine phosphorylation sites, Ser^{534} and Ser^{544}, are within well recognized CK2 motifs (34). This coincides with earlier observations that calnexin in microsomes was *in vitro* phosphorylated by CK2 (14, 15) and that CK2 was purified as an ER membrane-associated kinase (14). The identification of a third site of calnexin phosphorylation (Ser^{563} in HepG2; Ser^{564} in MDCK) was not predicted from previous *in vitro* studies (1, 14, 15). This site, invariant in mammalian calnexins, is within a motif potentially recognized by either PKC (35, 36) or PDK (37, 38).

We have presented evidence for diphosphorylated and triphosphorylated (Figs. 7 and 8) calnexins but no conclusive data for a monophosphorylated form, *i.e.* with only one of the two CK2 sites or only the $S^{563}PR$ site being phosphorylated, since no singly phosphorylated fragments encompassing the three sites were identified. Nonphosphorylated peptides encompassing the observed two CK2 sites of serine phosphorylation were identified by DE-MALDI-ToF MS analyses: ^{532}QKSDAEEDGGTVSQEEEDRKPK^{553} of HepG2 calnexin and ^{535}SDAEEDGGTASQEEDDRKPK^{554} of MDCK calnexin (Figs. 2 and 3, and Table II). The strongest evidence for only one of the two CK2 sites being phosphorylated was observed from MDCK trypsinized calnexin (Fig. 3*A* and Table II). The peptide ion, *m/z* 2130.9 (Fig. 3*A* and Table II) corresponds to the partial tryptic fragment ^{533}pyro-QK**S**DAEEDGGTA**S**QEEDDR^{551}, containing one phosphate group and cyclization of the NH_2-terminal glutamine (calculated average mass, 2130.9) (52). The cyclization of the NH_2-terminal glutamine of this tryptic fragment was suggested also by Cala and co-workers (15). For both

[5] H. N. Wong, E. Chevet, A. W. Bell, D. Y. Thomas, and J. J. M. Bergeron, unpublished observations.

calnexins, the two phosphorylated CK2 sites (Ser^{534} and Ser^{544}, HepG2 calnexin) are contained within the same tryptic fragment, and thus by our strategies, these two phosphorylation sites could not be characterized individually. Evidence for a nonphosphorylated state of the most COOH-terminal serine residue was not obtained. This may be a consequence of complete proteolytic digestion of this nonphosphorylated form and subsequent loss of the corresponding tryptic tripeptide, (R)S^{563}PR, during desalting/washing steps prior to MS analyses. However, the S^{563}PR site in the diphosphorylated large partial tryptic fragment (Fig. 7) that contains three potential sites of phosphorylation may correspond to a nonphosphorylated Ser^{563} site. On this basis, there are six potentially different (three mono- and three diphosphorylated) partially phosphorylated states of calnexin that probably represent a regulatory mechanism for calnexin action.

The phosphorylation results presented in this paper extend the previous finding by Capps and Zuniga (17) and Le *et. al.* (16) that a significant proportion of calnexin was phosphorylated *in vivo*. The identification of phosphorylated calnexin in association with a subset of incompletely folded major histocompatibility complex class I allotypes (17) or of the misfolded null Hong Kong mutant of α-1-antitrypsin (16) is suggestive of a coincident and perhaps regulatory role with the action of the luminal domain of calnexin in glycoprotein folding and quality control. Conservation of the three serine targets of protein kinases as elucidated here predicts that this conservation and their phosphorylation are under strict control. Elucidation of the signaling cascades that trigger calnexin phosphorylation at the PKC/PDK site as well as the CK2 sites may lead to new insights in the regulation of cargo folding and transport from the ER. These studies may also lead ultimately to a rationale for the evolution of three distinct genes in mammals that encode this family of molecular chaperones.

Acknowledgments—We thank Dr. Louise Larose for advice and assistance in phosphoamino acid analysis and Pamela H. Cameron for technical assistance.

REFERENCES

1. Wada, I., Rindress, D., Cameron, P. H., Ou, W-J., Doherty, J. J., II, Louvard, D., Bell, A. W., Dignard, D., Thomas, D. Y., and Bergeron, J. J. M. (1991) *J. Biol. Chem.* **266,** 19599–19610
2. Ou, W-J., Bergeron, J. J. M., Li, Y., Kang, C. Y., and Thomas, D. Y. (1995) *J. Biol. Chem.* **270,** 18051–18059
3. Ou, W-J., Cameron, P. H., Thomas, D. Y., and Bergeron, J. J. M. (1993) *Nature* **364,** 771–776
4. Hammond, C., Braakman, I., and Helenius, A. (1994) *Proc. Natl. Acad. Sci. U. S. A.* **91,** 913–917
5. Bergeron, J. J. M., Brenner, M. B., Thomas, D. Y., and Williams, D. B. (1994) *Trends Biochem. Sci.* **19,** 124–128
6. Hebert, D. N., Foellmer, B., and Helenius, A. (1995) *Cell* **81,** 425–433
7. Ware, F. E., Vassilakos, A., Peterson, P. A., Jackson, M. R., Lehrman, M. A., and Williams, D. B. (1995) *J. Biol. Chem.* **270,** 4697–4704
8. Nauseef, W. M., McCormick, S. J., and Clark, R. A. (1995) *J. Biol. Chem.* **270,** 4741–4747
9. Peterson, J. R., Ora, A., Van, P. N., and Helenius, A. (1995) *Mol. Biol. Cell* **6,** 1173–1184
10. Rodan, A. R., Simons, J. F., Trombetta, E. S., and Helenius, A. (1996) *EMBO J.* **15,** 6921–6930
11. Helenius, A., Trombetta, E. S., Hebert, D. N., and Simons, J. F. (1997) *Trends Cell Biol.* **7,** 193–200
12. Zapun, A., Petrescu, S. M., Rudd, P. M., Dwek, R. A., Thomas, D. Y., and Bergeron, J. J. M. (1997) *Cell* **88,** 29–38
13. Zapun, A., Darby, N. J., Tessier, D. C., Michalak, M., Bergeron, J. J. M., and Thomas, D. Y. (1998) *J. Biol. Chem.* **273,** 6009–6012
14. Ou, W-J., Thomas, D. Y., Bell, A. W., and Bergeron, J. J. M. (1992) *J. Biol. Chem.* **267,** 23789–23796
15. Cala, S. E., Ulbright, C., Kelley, J. S., and Jones, L. R. (1993) *J. Biol. Chem.* **268,** 2969–2975
16. Le, A., Steiner, J. L., Ferrell, G. A., Shaker, J. C., and Sifers, R. N. (1994) *J. Biol. Chem.* **269,** 7514–7519
17. Capps, G. G., and Zuniga, M. C. (1994) *J. Biol. Chem.* **269,** 11634–11639
18. Schue, V., Green, G. A., Girardot, R., and Monteil, H. (1994) *Biochem. Biophys. Res. Commun.* **203,** 22–28
19. Tector, M., Zhang, Q., and Salter, R. D. (1994) *J. Biol. Chem.* **269,** 25816–25822
20. Just, I., Selzer, J., Wilm, M., von Eichel-Streiber, C., Mann, M., and Aktories, K. (1995) *Nature* **375,** 500–503
21. Boyle, W. J., van der Geer, P., and Hunter, T. (1991) *Methods Enzymol.* **201,** 110–149
22. Wilm, M., Shevchenko, A., Houthaeve, T., Breit, S., Schweigerer, L., Fotsis, T., and Mann, M. (1996) *Nature* **379,** 466–469
23. Betts, J. C., Blackstock, W. P., Ward, M. A., and Anderton, B. H. (1997) *J. Biol. Chem.* **272,** 12922–12927
24. Wilm, M., and Mann, M. (1996) *Anal. Chem.* **68,** 1–8
25. Wilm, M. S., and Mann, M. (1994) *Int. J. Mass Spectrom. Ion Processes* **136,** 167–180
26. Wilm, M., Neubauer, G., and Mann, M. (1996) *Anal. Chem.* **68,** 527–533
27. Carr, S. A., Huddleston, M. J., and Annan, R. S. (1996) *Anal. Biochem.* **239,** 180–192
28. Covey, T., Shushan, B., Bonner, R., Schroder, W., and Hucho, F. (1991) in *Methods in Protein Sequence Analysis* (Jornall, H., Hoog, J. O., and Gustavsson, A. M., eds.) pp. 249–256, Birkhaeuser Verlag, Basel, Switzerland
29. Appel, R. D., Bairoch, A., and Hochstrasser, D. F. (1994) *Trends. Biochem. Sci.* **19,** 258–260
30. Altschul, S. F., Gish, W., Miller, W., Myers, E. W., and Lipman, D. J. (1990) *J. Mol. Biol.* **215,** 403–410
31. Pearson, W. R., and Lipman, D. J. (1988) *Proc. Natl. Acad. Sci. U. S. A.* **85,** 2444–2448
32. Thompson, J. D., Higgins, D. G., and Gibson, T. J. (1994) *Nucleic Acids Res.* **22,** 4673–4680
33. David, V., Hochstenbach, F., Rajagopalan, S., and Brenner, M. B. (1993) *J. Biol. Chem.* **268,** 9585–9592
34. Pinna, L. A. (1990) *Biochim. Biophys. Acta.* **1054,** 267–284
35. Kishimoto, A., Nishiyama, K., Nakanishi, H., Uratsuji, Y., Nomura, H., Takeyama, Y., and Nishizuka, Y. (1985) *J. Biol. Chem.* **260,** 12492–12499
36. Woodgett, J. R., Gould, K. L., and Hunter, T. (1986) *Eur. J. Biochem.* **161,** 177–184
37. Nigg, E. A. (1995) *BioEssays* **17,** 471–480
38. Robinson, M. J., and Cobb, M. H. (1997) *Curr. Opin. Cell Biol.* **9,** 180–186
39. Feramisco, J. R., Glass, D. B., and Krebs, E. G. (1980) *J. Biol. Chem.* **255,** 4240–4245
40. Glass, D. B., el-Maghrabi, M. R., and Pilkis, S. J. (1986) *J. Biol. Chem.* **261,** 2987–2993
41. Covey, T. R., Bonner, R. F., Shushan, B. I., and Henion, J. D. (1988) *Rapid Commun. Mass Spectrom.* **2,** 249–256
42. Tjoelker, L. W., Seyfried, C. E., Eddy, R. L., Byers, M. G., Shows, T. B., Calderon, J., Schreiber, R. B., and Gray, P. W. (1994) *Biochemistry* **33,** 3229–3236
43. Ikawa, M., Wada, I., Kominami, K., Watanabe, D., Toshimori, K., Nishimune, Y., and Okabe, M. (1997) *Nature* **387,** 607–611
44. Opas, M., Dziak, E., Fliegel, L., and Michalak, M. (1991) *J. Cell Physiol.* **149,** 160–171
45. Watanabe, D., Yamada, K., Nishina, Y., Tajima, Y., Koshimizu, U., Nagata, A., and Nishimune, Y. (1994) *J. Biol. Chem.* **269,** 7744–7749
46. Tanaka, H., Ikawa, M., Tsuchida, J., Nozaki, M., Suzuki, M., Fujiwara, T., Okabe, M., and Nishimune, Y. (1997) *Gene* (*Amst.*) **204,** 159–163
47. Rajagopalan, S., Xu, Y., and Brenner, M. B. (1994) *Science* **263,** 387–390
48. Sonnichsen, B., Fullekrug, J., Van, P. N., Diekmann, W., Robinson, D. G., and Mieskes, F. (1994) *J. Cell Sci.* **107,** 2705–2717
49. Parlati, F., Dignard, D., Bergeron, J. J. M., and Thomas, D. Y. (1995) *EMBO J.* **14,** 3064–3072
50. Parlati, F., Dominguez, M., Bergeron, J. J. M., and Thomas, D. Y. (1995) *J. Biol. Chem.* **270,** 244–253
51. Schaller, J., Pellascio, B. C., and Schlunegger, U. P. (1997) *Rapid. Commun. Mass Spectrom.* **11,** 418–426
52. Allen, G. (1989) in *Sequencing of Proteins and Peptides* (Burdon, R. H., and van Knippenberg, P. H., eds) 2nd Ed., Elsevier Science Publishing Co., Inc., New York

Conserved *in Vivo* Phosphorylation of Calnexin at Casein Kinase II Sites as Well as a Protein Kinase C/Proline-directed Kinase Site

Hetty N. Wong, Malcolm A. Ward, Alexander W. Bell, Eric Chevet, Satty Bains, Walter P. Blackstock, Roberto Solari, David Y. Thomas and John J. M. Bergeron

J. Biol. Chem. 1998, 273:17227-17235.
doi: 10.1074/jbc.273.27.17227